Collecting Performance of a Lidar Telescope at Short Distances

K. Ohm

Alfred Wegener Institute for Polar and Marine Research,
Section Marine Physics, D-27568 Bremerhaven, Germany

R. Willkomm

Carl von Ossietzky University, Physics Department, P.O.Box 2503,
D-26111 Oldenburg, Germany

ABSTRACT

The telescope of a depth resolving ship-board Lidar system has the task to collect radiation from a range of distances and to concentrate it on a photomultiplier tube (PMT). The radiation occurs from matter irradiated by the laser. The sensitivity of the system is calculated and proves to be a function of depth of the observed matter. The sensitivity function has its maximum at an intermediate distance between an assumed maximum depth of observation and zero. The smaller sensitivity in the proximity of the telescope helps to compress the huge dynamic signal range, a characteristic of a Lidar system operated in the sea. By means of the given formulae a Lidar telescope can be optimized.

INTRODUCTION

A ship-board Lidar for observations of particulate and dissolved matter distributed in a seawater column is vertically mounted in the ship's hull and looks downward through a quarz glass window. A general description of such a time resolving system is presented in this volume (Reuter et al.,1994) while this paper deals especially with the design of the optical components of a Lidar of this type. Harms et al. (1978) performed similar calculations concerning a Lidar system for the atmosphere. Their results are similar but are not directly applicable to the system under consideration, as they cover a distance range of 100m to 10km, whereas in the sea a range of 2m to 60m is of interest.

The interaction of a laser pulse with matter in a certain depth induces upwelling radiation. Its properties as the wavelength and the intensity characterize the composition and the concentration of the matter, whereby the exciting wavelength has to be taken into account. In this article it is not necessary to distinguish between different processes such as the Raman effect of water, the Mie scattering of particles and the fluorescence of chlorophyll and yellow substances. The efficiency ρ of any interaction is determined by the product of concentration and effective cross section. By means of the time resolution of the received signal the distance of the matter from the Lidar is evaluated, and the amplitude contains information of the concentration of matter. The amplitude is predominantly determined by the sensitivity of the optical setup which has to be known for the evaluation of the data and for optimizing of the system.

If an interaction takes place in a certain depth z, then ρ is the ratio of the diffuse upwelling radiant intensity and the downwelling radiant flux. The downwelling flux is attenuated along its path, and the amount of transmitted flux is expressed by the factor of transmission T_d. Correspondingly T_u is the transmission of the upwelling flux. Both factors depend on the wavelength, but this detail has no consequences in this respect, and it is not specially adressed.

Using the Lidar for investigations in the water column has consequences for the design of the optical components. The main part is the telescope of the receiver. Normally a telescope forms an image of faraway radiant sources, but in this case a radiant flux has to be collected also from the immediate proximity. The aim of the design of the ray path is not to form a sharply defined image but light collection and its optimisation. Especially the knowledge of the sensitivity of the telescope as a function of depth or distance is useful for data interpretation and is necessary for the optimal design of the system.

METHOD

In the above first section the effects concerning the interaction of radiation with matter are roughly described. In the following the whole ray path of the Lidar system will be traced quantitatively to derive a precise definition of the sensitivity.

The laser excites with a radiant flux ϕ_1, and the receiver collects the flux ϕ_r, which is

$$\phi_r = \phi_1 \, T_d \, \rho T_u \, S\,(z) \tag{1}$$

In this simplified Lidar equation T_d, ρ and T_u characterize the optical properties of the water with its dissolved and suspended matter, while $S(z)$ spezifies the optical setup. We define

$$S\,(z) = \frac{\phi_{ra}}{\phi_1}\,\mathrm{sr} \tag{2}$$

as the sensitivity of the optical setup. Here ϕ_{ra} is the radiant flux collected by the receiver during an imaginary experiment in air instead of water. In air we have $T_d = T_u = 1$ and we assume $\rho = 1\mathrm{sr}^{-1}$. Because $S(z)$ has the dimension of a solid angle, the unit sr will be applied in the appropriate equations when it is necessary.

With the known sensitivity function $S(z)$ the data processing and interpretation can be done stepwise with the following procedure. With increasing z equation (1) is solved for ρ with the known signals ϕ_1 and ϕ_r and the function $S(z)$. T_d and T_u are derived from the integrated local attenuation coefficients which depend in their turn on $\rho\,(z)$. Besides the calculation of $S(z)$ the function can be measured by means of an experiment in air which yields $T_{d,u} = 1$. The process characterized by ρ is assumed to take place on a diffuse reflecting surface with constant properties. The constant has not necessarily to be $\rho = 1\mathrm{sr}^{-1}$, as assumed above, because its value is unimportant when the measured data are normalized. If the Raman signal is measured additionally with the other properties, the sensitivity must not necessarily be known, because the normalization is done in all different depths and comprises the function $S(z)$. For more details see (Reuter et al., 1994).

The telescope of a Lidar device normally is designed as a reflector type. But for the purposes of calculation and explanation a refractor is more convenient, and as the results are not affected by the type of telescope this paper deals with a Kepler refractor. Consequently the objective is referred to as the *front lens* or the *lens* instead of the parabolic mirror used in reality. This mirror shows only negligible aberrations for light rays nearly parallel to the axis. For this reason the computation uses the simplified thin-lens equation.

This study will get a more universal validity if the construction of the PMTs as a part of the receiver does not affect the calculation. This can be achieved by a ray path, which leads all radiation to the PMT which had already passed the field stop. Then the calculation deals only with the system objective and field stop.

Figure 1 demonstrates the ray path under consideration. Some basic dimensions are preliminary settled, such as the diameter of the lens $2L$, its focal length f and the beam divergence of the laser β. Generally, the field stop with the radius D is not placed in the focal plane but usually in a greater distance d from the lens. Consequently the entrance window (which is the image of the field stop) has a finite distance z_0 in the object space. At this distance the area $A_{\rho\,0} = \pi\, R_0^2$ is fully irradiated by the laser and it is imaged into the field stop. The radius of the field stop follows the equation

$$D \geq R_0\, d / z_0 = R_0\,(d-f)/f \tag{3}$$

With the smallest diameter the diaphragm and the image of $A_{\rho\,0}$ have the same size. R_0 is determined by the beam divergence β. If for example the radiation source is assumed in the centre of the lens,

$$2\,R_0 = \beta\, z_0 \tag{4}$$

is applied. Assuming a certain d, the particular depth z_0 is established from where radiation out of the whole area $A_{\rho\,0}$ passes the total area of the lens and also of the diaphragm.

Now the sensitivity $S(z)$ can be calculated. As already mentioned, T_d and T_u are assumed to be equal to one. In this case the radiant flux of the laser ϕ_1 hits an area A_ρ at depth z as incident flux. On assuming a homogeneous intensity distribution the irradiance is the quotient of ϕ_1 and A_ρ. From the diffuse reflection with $\rho = 1\mathrm{sr}^{-1}$ results a non directional radiance $\phi_1/(A_\rho\, sr)$. This radiance multiplied by the area da and the solid angle Ω forms the radiant flux $d\,\phi_{ra}$ through the diaphragm.

$$d\,\phi_{ra} = \phi_1\,\Omega/(A_\rho\,\mathrm{sr})\,da \tag{5}$$

In figure 2 is depicted that the radiation coming out of the solid angle Ω passes the lens and the diaphragm. Ω is formed by the area A_L and z, where A_L is that part of the lens, which contributes to the signal.

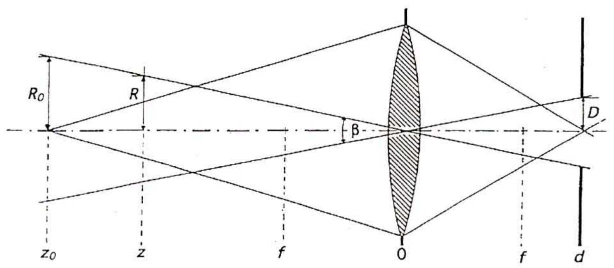

Fig. 1 - Objective and field stop of the telescope. The beam divergence β is the same as the angular field of view. In this case the sign of equality holds in equation (3).

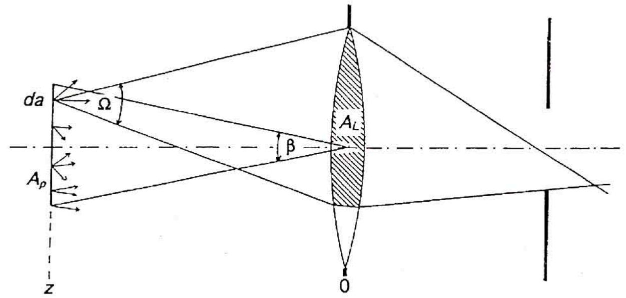

Fig. 2 - The contributing area A_L of the lens together with the distance z forms the solid angle Ω, in which a part from the diffuse radiation coming out of the area da is collected.

$$\Omega = A_L/z^2 \quad (6)$$

The contributing area A_L depends on the distance of the area da from the axis. With equation (6) the solid angle becomes a funtion of r, $\Omega = \Omega\,(r)$. The calculation of this function will be done later with the equations (9)-(11).
Now equation (5) can be integrated:

$$S\,(z) = 1/A_p \int_{A_p} \Omega\,(r)\,da$$

With the circular area $da = 2\,\pi\,r\,dr$ we obtain

$$S\,(z) = 2/R^2 \int_0^R \Omega\,(r)\,r\,dr \quad (7)$$

The sensitivity depends on z, while the right hand side of this equation shows a function depending on R. z and R are related by the laser beam divergence β. In the above mentioned simple case, where a point source is located in the lens, we get

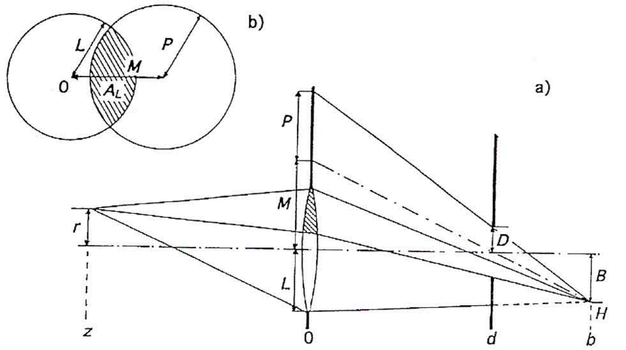

Fig. 3a - The diaphragm is projected from the centre H into the plane of the lens. The central point has the distance M from the axis, and the radius of the circle is P. Only the pencil of rays, which penetrates the hatched area of the lens, contributes to the signal. b) The intersection area A_L formed by the rim of the lens and the projected diaphragm is calculated with the equations (9)-(11).

$$2\,R = \beta\,z \quad (8)$$

If an equation of this type is inserted in equation (7) the dependence on z can be seen directly.
For the numerical evaluation of the integral equation (7), the knowledge of the contributing area A_L as a function of the distance r has to be calculated. The method is to project the diaphragm back into the principal plane of the lens. Here the intersection area A_L has to be calculated from the projected diaphragm and the rim of the lens. Centre of the projection is the image H in figure 3. Its coordinates evaluated by means of the lens equation are

$$b = z\,f/(z-f)\ , \qquad B = r\,f/(z-f) \quad (9)$$

The centre of the projected diaphragm has the distance M from the axis, and the radius of the projected diaphragm is P as displayed in figure 3.

$$M = B\,d/(b-d)\ , \qquad P = D\,b/(b-d) \quad (10)$$

The intersection area A_L can be computed by the following equation:

$$\begin{aligned} A_L = {} & L^2\,arccos\,(\,(M^2 + L^2 - P^2)/(2\,ML)\,) \\ & + P^2\,arccos\,(\,(M^2 - L^2 + P^2)/(2\,MP)\,) \\ & - 1/2\,(4\,L^2\,M^2 - + (M^2 + L^2 - P^2)^2\,)^{1/2} \end{aligned} \quad (11)$$

With the equations (3)-(6) and (8)-(11) all tools are now available for the numerical evaluation of equation (7). Once the beam divergence β of the laser, the optical parameters L and f, and a distance of the diaphragm d have been chosen, z_0 results from the right hand side of equation (3). R_0 follows from equation (4), and the radius of the diaphragm D from the left hand side of equation (3), for the present with the sign of equality being valid. The result of all computation will be the sensitivity S in a number of distances z. The above algorithm needs the image point H. Therefore the minimum distance z must be greater than f which means no restriction with a reflector of the Kepler type.

RESULTS

The first computations were done with data of commercially available parts with the following specifications:

L = 0.1 m f = 1.2 m β = 2.4 mrad

For three distances of the diaphragm the calculations result in the following table.

d/m	z_0/m	R_0/mm
1.25	30	36
1.2329	45	54
1.2245	60	72

The corresponding diameter of the diaphragm is $2D = 3$ mm. The function $S(z)$ is shown in figure 4 with these three distances as parameter. At greater distances z the sensitivity decreases with increasing z, as expected. At z_0 the function shows a kink, at smaller distances a maximum, and surprisingly a decrease with shorter distances from the telescope. The sensitivity in the kink point at z_0 is the highest possible at this distance, if the variation is done by displacing the diaphragm. Its value is

$$S(z_0) = \pi L^2 \cdot \mathrm{sr}/z_0^2 \qquad (12)$$

This decrease in the proximity of the telescope is a useful effect, if it is taken into account that due to the attenuation the radiant flux is diminished according to Lambert's law:

$$T_{d,u} = 1 - C_{d,u} = e^{-cz}$$

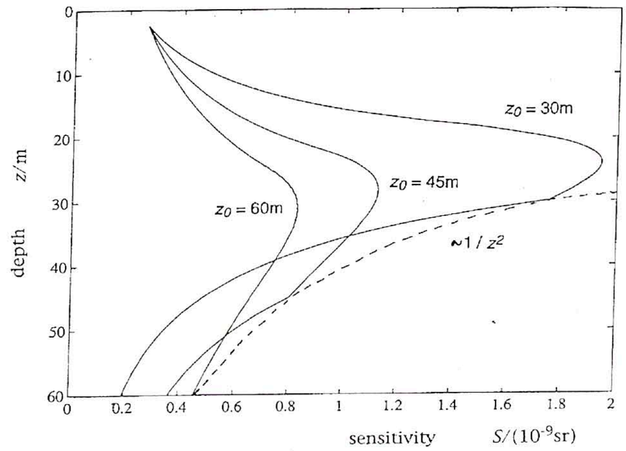

Fig. 4 - The sensitivity $S(z)$ for three different distances z_0. The positions of the kink points follow from the equation (12) and describe the highest achievable sensitivity at these distances.

In figure 5 the sensitivity is computed with $d = 1.25$m and for different attenuation coefficients c of the water in front of the telescope. Even in the purest water and at wavelengths of the optical window the signal arising out of 20m to 25m distance has only half of the strength compared with that in air, and with an attenuation coefficient of $c = 0.08\mathrm{m}^{-1}$ the maximum of the sensitivity has totally disappeared. The dynamic range of the signal, which is always a problem in such a Lidar system, is helpfully compressed. As a consequence of the light attenuation the greatest possible sensitivity is needed in the greatest depth from where data are expected. For that reason the diaphragm is aligned in a distance d greater than f, so that the corresponding depth z_0 is the maximum depth of observation.

To increase the sensitivity further the lens must be enlarged according to equation (12). But this is limited due to the

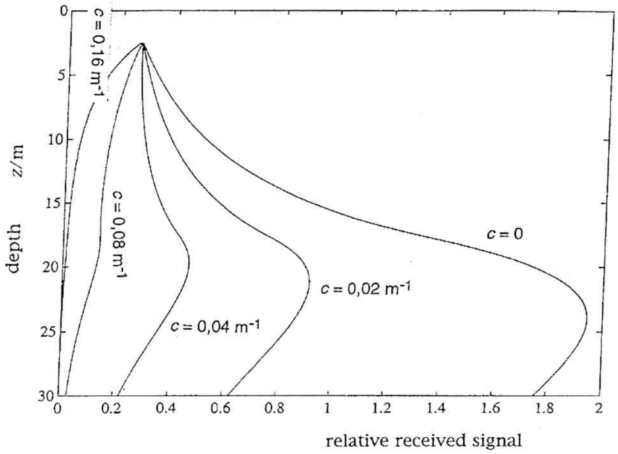

Fig. 5 - For z_0 = 30 m the relative signal of a Lidar is shown, when attenuating matter is introduced. The curve with the attenuation coefficient c = 0 is the same as in figure (4).

costs or the mechanical dimensions of the apparatus. Another method was evaluated, namely whether it would help to enlarge the diaphragm with the corresponding expanded laser beam divergence. Figure 6 shows that in this case the sensitivity at z_0 is not changed, but the telescope gets more sensitive at closer distances. The maximum of the sensitivity migrates closer to the telescope where it is of no use. With enlarged diaphragm and beam divergence one counteracts the signal compression by generating a higher sensitivity in the near field.

For practical reasons the diameter of the diaphragm should be made somewhat larger than the image of the area $A_{\rho\,0}$. By doing this clearance is available to account for tolerances of the mechanical parts and inaccuracies of the alignment. The

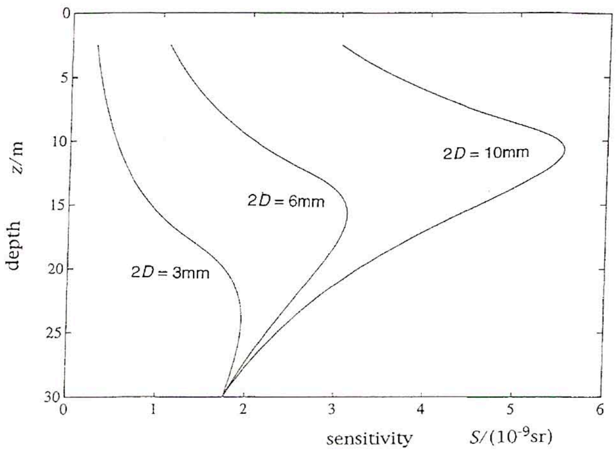

Fig. 6 - The sensitivity $S(z)$, computed with three different diameters of the diaphragm $2D$ = 3 mm, 6 mm and 10 mm and with z_0 = 30m, with the laser beam divergence correspondingly larger to illuminate the whole image of the diaphragm in the object space.

consequences are demonstrated in figure 7. The left line computed with the minimum diameter is already known. With a larger diaphragm but constant beam divergence the sensitivity increases in the near field similar to the preceeding example. As a conclusion for the diameter $2D$ the greater sign in equation (3) is valid but without overdoing. The precise value depends on the construction.

The reflector telescope realized on the basis of the above mentioned principles and computations utilizes a secondary mirror to direct the signal out of the main tube of the telescope. This plano reflector positioned under 45° serves as the field stop at the same time. On its back side directed to the object space there is another mirror, reflecting the laser beam into the optical axis of the system. These components form a shield around the axis for radiant flux out of the object space. Computed with the above described method these mirrors lead to an additional decrease of the sensitivity immediately in front of the telescope. This effect depends strongly on the individual dimensions of the design and was treated in detail by Harms (1979). Therefore it will not be discussed in this paper no more than the small variations resulting from a more realistic description of the laser beam. Its diameter in front of the telescope is 8mm, thus the beam would start from an imaginary point source in the image space in a distance l = 3.3m from the lens. Equation (8) then alters in

$$2R = \beta z + \beta l \tag{8a}$$

Besides the outlined experiment with a reflecting surface there exists another way of how to measure the sensitivity function. Assuming the air outside the laboratory's window contains homogeneously distributed aerosoles, the time resolved signal, induced by a single laser pulse out of the window into the open air returnes the function $S(z)$.

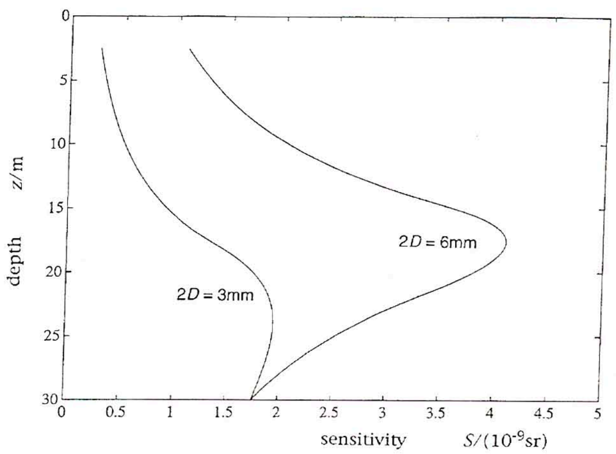

Fig. 7 - A similar computation as in figure 6, with two diameters, but the laser beam divergence is kept small. The increased sensitivity at shorter distances has to be accepted for tolerances of the mechanical parts.

Only the time scale has to be converted according to the different light velocities in air and in water. Such a result is shown in figure 8.

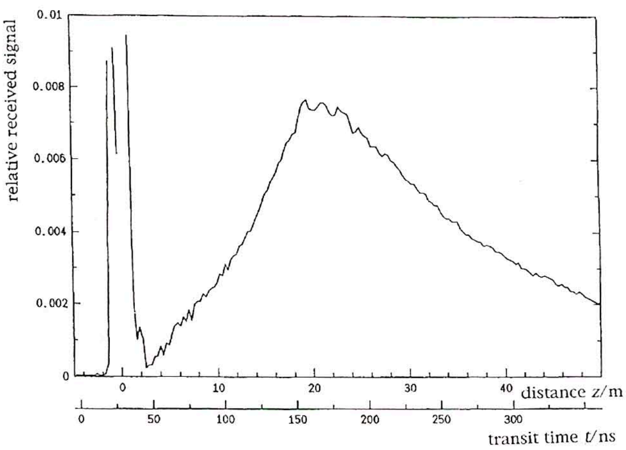

Fig. 8 - An example of the Lidar signal when operating into the atmosphere. The strong signal around z = 0 is due to reflexions within the telescope itself. Assumed homogeniously distributed aerosols this signal returns the function of the sensitivity.

CONCLUSION

With the derived method the sensitivity function of a Lidar telescope can be computed. This allows to optimize the optical setup of a Lidar system. It is necessary to achieve the highest possible sensitivity in a certain maximum depth z_0, because the light attenuation diminishes the radiation exponentially with the path length. Most effective is the choice of the greatest diameter of the lens or mirror of the telescope. But the diameter is limited in view of the costs and the space available in the ship's hull. A further arrangement is to designate the maximum distance z_0, where a disc is radiated by the laser beam and from where a signal is expected. If the field stop is put into the plane of the image of this disc and the diameter of the diaphragm is made somewhat larger to provide for tolerances, the highest possible sensitivity in the maximum depth is achieved. With shorter distances the sensitivity increases to a maximum and decreases in the proximity of the telescope. This trend helps to compress the huge dynamic range of the Lidar signals and is a useful support.

The sensitivity of the Lidar telescope is not affected directly by the relative aperture of the lens. But the precondition of this computation, namely that all radiation which passed the diaphragm must reach the PMT, implies an influence of the relative aperture on the sensitivity. As an explanation a hint at the eyelens of the telescope may be sufficient. This second lens forms an image of the diaphragm on the PMT. Its relative aperture must be slightly greater than the objective and its diameter is limited by mechanical reasons. From the surface area of the PMT and a minimum distance in the receiver unit a maximum diameter of the diaphragm may result which gives an upper limit for the focal length of the objective. As the beam divergence of the laser and the diameter of the lens $2L$ are already fixed, a minimum relative aperture is required.

A laser with a small beam divergence has to be used, by no means should it be enlarged artificially. Following these rules the smallest possible volume is irradiated and observed by the telescope. This minimizes stray light from the background and improves the Lidar signal.

REFERENCES

Harms, J.,1979, Lidar return signals for coaxial and noncoaxial systems with central obstructions. Applied Optics,18, 1559-1566.

Harms, J., Lahmann, W., and Weitkamp, C., 1978, Geometrical compression of lidar return signals. Applied Optics, 17, 1131-1135.

Reuter, R., Willkomm, R., Krause, G. and Ohm, K., 1994, Development of a Shipboard Lidar: Technical Layout and First Results. EARSeL Advances in Remote Sensing, paper included in this volume.